# Large differences in the optical properties of a single layer of Si on Ag(110) compared to silicene

Yves Borensztein,[1,2,*] Geoffroy Prévot,[1,2] and Laurence Masson[3]

[1]*Sorbonne Universités, UPMC Univ Paris 06, UMR 7588 Institut des NanoSciences de Paris, 4 place Jussieu, F-75005 Paris, France*

[2]*CNRS, UMR 7588 Institut des NanoSciences de Paris, F-75005 Paris, France*

[3]*Aix Marseille Université, CNRS, CINaM UMR 7325, F-13288 Marseille, France*

(Received 28 March 2014; revised manuscript received 12 May 2014; published 9 June 2014)

The optical properties of Si nanoribbons grown on Ag(110) under ultrahigh vacuum have been experimentally determined by use of *in situ* surface differential reflectance spectroscopy. Real-time measurements showed a clear transition of the optical response of the Si deposit at full coverage of the Ag(110) surface, corresponding to 0.8 monolayer of silicon. The spectra measured for the complete self-assembled nanoribbon layer are different from the reflectance spectrum calculated for a layer of silicene on silver, which rules out the possible silicenelike character of this layer. Furthermore, the dielectric function of the nanoribbons is calculated from the experimental data and is similar to the one of amorphous silicon, with a red shift of about 0.6 to 0.8 eV of the main absorption feature. This result indicates that the Si nanoribbons display a preferential $sp^3$ hybridization as in amorphous Si and not a partial $sp^2$ hybridization as expected for silicene.

DOI: 10.1103/PhysRevB.89.245410 PACS number(s): 78.20.Ci, 78.67.−n, 78.68.+m

## I. INTRODUCTION

The large interest in graphene layers and their applications has motivated scientists to investigate other group-IV two-dimensional (2D) layers that would be analogous to graphene, i.e. with honeycomb structure and $sp^2$ bonding. Among these, silicene, a single sheet of silicon, would be the best candidate for potential use in electronics. Although there is no equivalent of graphite for silicon, 2D epitaxial layers can be grown on some crystal surfaces: Ag(110) [1], Ag(111) [2], $ZrB_2$(0001) [3], or Ir(111) [4]. For Si layers grown on Ag(110) and Ag(111), a band structure similar to the one of graphene was inferred from angle-resolved photoemission spectroscopy (ARPES) experiments, where a band dispersion resembling the Dirac cones for graphene was observed [5,6]. For Ag(110), density functional theory (DFT) calculations also concluded to a distorted honeycomb structure for the Si layer [5]. However, these observations have recently been reconsidered. Scanning tunneling microscopy (STM) and grazing incidence x-ray diffraction (GIXD) experiments have shown that the honeycomb model computed by DFT is not adapted since the Ag(110) exhibits a missing-row reconstruction upon Si adsorption [7]. At the same time, another experimental study concluded that the honeycomb structure observed by STM on Si/Ag(110) was due to tip artifacts [8], and a theoretical study of the electronic structure of Si/Ag(110) and Si/Ag(111) showed that the conical features visible in ARPES measurements are not due to silicon but to the silver substrate, as an effect of band folding induced by the Si overlayer periodicity [9]. Thus, whereas there is no absolute proof of the nonexistence of silicene grown on Ag(110), there is no true experimental evidence of the $sp^2$ bonding of Si atoms in the 2D Si epitaxial layers.

Important information on the existence of silicene can be obtained from optical measurements, since the optical responses of graphene, silicene, or germanene are directly related to their electronic band structure. In particular, due to the existence of the Dirac cone, the infrared absorption of these 2D layers has been shown to be equal to $\pi\alpha = 0.0230$ at small energies, where $\alpha$ is the Sommerfeld fine structure constant. This has been predicted for three of them [10,11] and proved experimentally for graphene [12–14]. Bechstedt *et al.* have determined the optical response of silicene by using *ab initio* methods based on DFT [10,15,16]. Figure 1 shows the optical absorption calculated for freestanding buckled silicene, from Ref. [16]. Similarly to the case of graphene, the absorption is equal to $\pi\alpha$ at small energies and also displays an intense feature at around 2 eV due to electronic transitions between $\pi$ and $\pi^*$ states. This transition is located at a much smaller energy than the similar one in graphene, for which it is observed at 4.6 eV [12,14] and calculated between 4 and 5 eV [10,11,16]. This position of 2 eV is also quite below the Ag interband edge located around 3.8 eV [17], which should favor its optical observation for Si grown on Ag(110). A second interband transition occurs at 4.8 eV.

Optical measurements appear, therefore, as a method of choice to study Si single layers and to determine their possible silicene character. However, contrary to graphene, such Si overlayers are grown on opaque single crystals (Ag, Ir, or $ZrB_2$ grown on Si) which prevents one from probing their optical absorption by transmittance measurements. In contrast, the reflectance of opaque substrates can be measured and, combined with differential methods, can be sensitive to small amounts of silicon. Surface differential reflectance spectroscopy (SDRS), which provides the relative change in reflectance of the sample due to the presence of additional atoms or molecules on the surface, has been shown to be an efficient technique to study adsorption phenomena [18,19], growth of very thin films on such substrates [20–22], and also to follow their kinetics [23,24].

Si epitaxial layers can easily be grown on Ag(110). When Si is deposited on the Ag(110) surface held at a temperature between 430 and 490 K, it has been shown that long nanoribbons (NRs) are forming, aligned along the $[1\bar{1}0]$ direction [1]. At these temperatures, both single NRs with a lateral size of 0.8 nm (i.e. two times the Ag lattice parameter) and double NRs are formed, the latter becoming

*Corresponding author: borensztein@insp.jussieu.fr

 

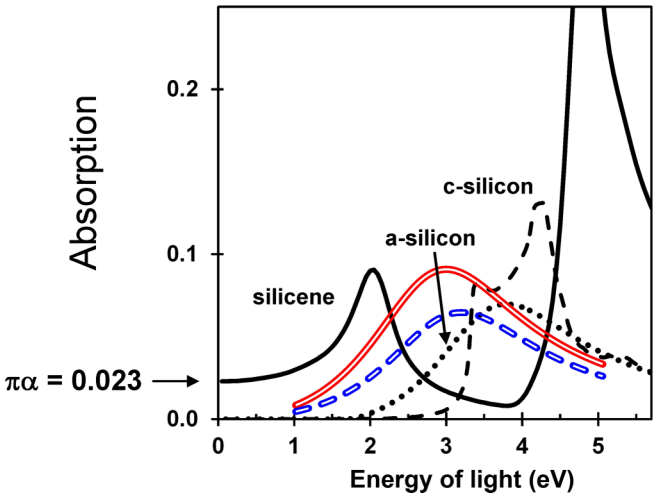


FIG. 1. (Color online) Optical absorption of a silicene layer [16] (black continuous line), of a crystalline Si layer [32] (black dashed line), of an amorphous Si layer [33] (black dotted line) for the same amount of Si atoms. Absorption of a 1 FC Si SANR layer on Ag(110) determined from the SDRS measurements performed between 1 and 5 eV, parallel to the NRs (red double line) or normal to the NRs (blue dashed double line).

the majority at 490 K. They self-assemble and eventually form a well-ordered array depending on the growth temperature, having locally either a $p(5\times2)$ or $c(10\times2)$ structure (denoted hereafter "×2"). These self-assembled nanoribbons (SANRs) cover the entire surface at a full coverage (FC) corresponding to 0.8 monolayer (ML), where 1 ML corresponds to the Ag(110) surface atom density, i.e. 8.45 atoms/nm$^2$ [7]. For higher coverages, the ×2 reconstruction is progressively replaced by a $c(8\times4)$ superstructure (denoted hereafter "×4") [8]. The aim of this paper is to investigate the optical response of Si single layers grown on Ag(110) and to compare it with the one expected for a silicene layer. We have followed *in situ* the surface differential reflectance (SDR) of Ag(110) during Si deposition at 450 K. After the description of the experimental details, the real-time monitoring of the SDR signal is presented which shows a sudden change at the $\times2 \rightarrow \times4$ transition. Then the optical response of the FC Si layer is discussed, compared to silicene, and analyzed by the use of an adapted dielectric function.

## II. EXPERIMENTAL

The experiments were performed in an ultrahigh vacuum chamber with a base pressure less than $10^{-10}$ mbar. The Ag(110) sample was prepared by repeated cycles of $Ar^+$ sputtering and annealing at 770 K. The cleanliness and the quality of the surface were controlled by a cylindrical mirror analyzer Auger electron spectrometer (AES) and by a spot profile analysis low-energy electron diffractometer (SPA-LEED). Si was evaporated at a rate of 0.03 ML/min from a Si wafer piece heated by direct current and deposited on the Ag substrate held at 450 K. The Si flux was determined by combining the SPA-LEED results and the AES measurements, with an accuracy estimated to be equal to 10%.

For the experiments presented here, completion of the first Si overlayer (1 FC) was determined from the measurement of the intensity of the ×2 superstructure SPA-LEED spots as a function of coverage. The corresponding maximum was found for the AES Si (92 eV)/Ag (356 eV) peak intensity ratio of 0.25. The temperature of 450 K used here, as checked by SPA-LEED, leads at this coverage to a well-organized ×2 layer and allows one to avoid or to reduce the additional three-dimensional Si nanostructures which are observed at 490 K [8]. For amounts higher than 1 FC, SPA-LEED shows the progressive fading of the ×2 superstructure and the appearance of the ×4 one.

The temperature was measured by a thermocouple located close to the sample on the sample holder, and the increase of temperature was less than 3 K during the evaporation time. The SDRS measurements were performed in the 1.1–5.5 eV optical range by use of a commercial spectrometer Maya from Ocean Optics. The SDR signal corresponds to the relative change of reflectance of the sample caused by the Si deposit and is defined by

$$\frac{\Delta R}{R} = \frac{R_{\mathrm{Ag}} - R_{\mathrm{Si/Ag}}}{R_{\mathrm{Ag}}}, \qquad (1)$$

where $R_{\mathrm{Ag}}$ and $R_{\mathrm{Si/Ag}}$ are the optical reflectances of the clean and the Si-covered Ag sample measured in normal incidence. The light was linearly polarized, with polarization either parallel or perpendicular to the $[1\bar{1}0]$ direction of the substrate. Surface differential reflectance was measured in the whole optical range during Si evaporation, at a rate of one spectrum every 10 s, and allowed us to real-time monitor the kinetics of formation of the Si layer.

## III. REAL-TIME OPTICAL MEASUREMENTS

The evolution of the SDR signal is shown in Fig. 2 as a function of the Si coverage measured in FC units, for different chosen energies of light and for polarization parallel to the Si NRs. Anticipating the next paragraph where the experimental SDR spectra displayed in Fig. 3(a) are discussed, the values

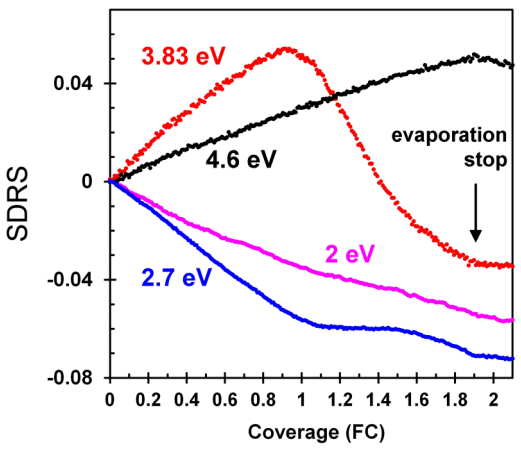


FIG. 2. (Color online) Evolution of the SDR signal for polarization along the NRs ($[1\bar{1}0]$ direction) as a function of the Si coverage, at four energies of light: 2 eV (purple), 2.7 eV (blue), 3.83 eV (red), and 4.6 eV (black).

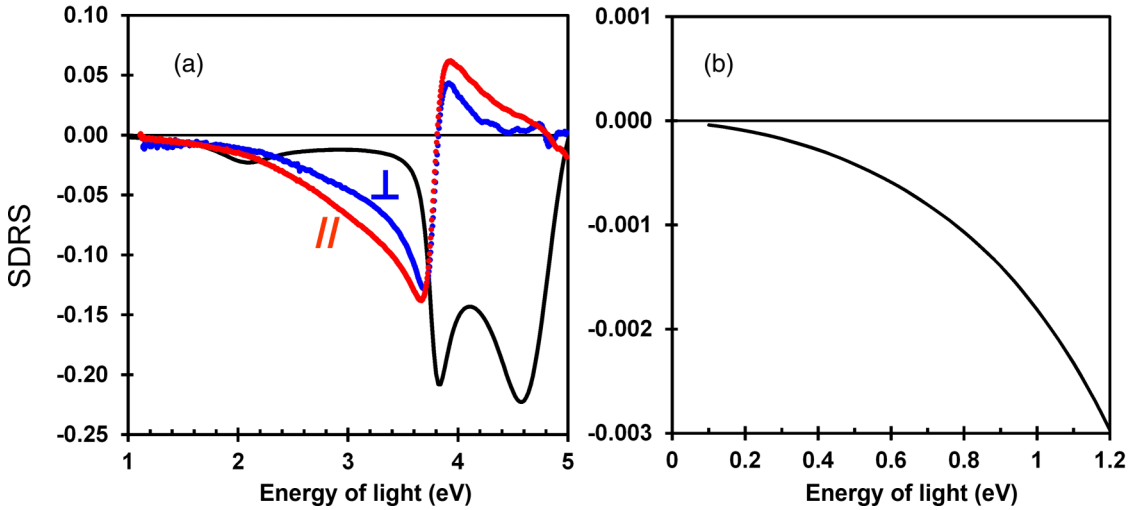


FIG. 3. (Color online) (a) Surface differential reflectance spectra measured for 1 Si FC on Ag(110). Red: light polarization along $[1\bar{1}0]$; blue: light polarization perpendicular to $[1\bar{1}0]$. The black line is the calculation using the dielectric function of silicene, from Ref. [16]. (b) Zoom of the calculated SDR spectrum in the low-energy range.

of 2.0 and 4.6 eV are linked to the expected peaks related to the absorption peaks of freestanding silicene. The energy of 2.7 eV corresponds to a broad feature between 2 and 3.6 eV observed in the experimental SDR spectra [see Fig. 3(a)], while the value of 3.83 eV is close to the position of a sudden change of the signal (going from negative to positive values), and is very sensitive to any change of the optical response of the overlayer.

The signals at 2.7 and 3.83 eV evolve approximately linearly up to about 1 FC, where a sudden change of slope is visible. On the contrary, no change of slope at any coverage is present at 4.6 eV, and only a tiny effect is seen at 2.0 eV, at the light energies where the main optical features of silicene should be observed. The almost linear evolution of the signal for 2.7 and 3.83 eV up to 1 FC can be associated with the known formation of the NRs at 450 K [7]: for coverages below saturation, very long NRs form on the surface, whose number increases with the Si coverage. Most of them are double NRs, and some are self-assembled, forming local $\times 2$ areas. By increasing the coverage, the $\times 2$ areas progressively enlarge until completion of the full SANR layer. No important change of the optical response is expected during this formation, and this could explain the evolution of the signal up to completion of the $\times 2$ SANR layer at 1 FC. For a coverage higher than 1 FC, the initial Si layer progressively transforms into a $c(8\times 4)$ superstructure [8]. This progressive transition from the $\times 2$ superstructure to the $\times 4$ one, after completion of the SANR layer, is expected to give rise to a different evolution of the optical response of the Si-covered surface and therefore explains the observed important changes of slopes at 1 FC for the signals at 2.7 and 3.83 eV. For higher coverage, the slopes at both energies change progressively above 1.5 FC. This could be the indication of an additional change of structure during the formation of the second layer. From the evolution of the SDR signal displayed in Fig. 2, it can be concluded that the transition between the $\times 2$ and the $\times 4$ structures is clearly seen in real-time SDRS measurements at 1 FC coverage.

## IV. SANR FULL COVERAGE

In this paragraph, we focus on the SDR spectra measured for the $\times 2$ superstructure at the SANR saturation. Figure 3(a) shows the SDR spectra for 1 FC of silicon deposited on Ag(110) at 450 K and measured at the same temperature, for polarizations of light parallel and perpendicular to the $[1\bar{1}0]$ direction. Both spectra display similar features, with a slightly higher intensity for light polarized along the NRs. The sharp derivativelike feature around 3.8 eV is due to the very deep minimum in the reflectance $R_{\mathrm{Ag}}$ of Ag, which enhances the effect on the SDR signal of any deposited layer, due to the presence of $R_{\mathrm{Ag}}$ at the denominator in Eq. (1). In order to determine whether these SDR spectra are compatible with the possible silicene character of the Si deposit, they have to be compared with the expected spectrum for silicene. The SDR signal for a material layer of thickness $d$ on a substrate can be expressed at first-order in $d/\lambda$ as a function of the dielectric function of the substrate $\varepsilon_{\mathrm{sub}}(\omega)$ and of the dielectric response of the layer, having dimension of length and generally described by a tensor $\Delta \overleftrightarrow{\varepsilon}(\omega)$ [25]. It reads for normal incidence with light polarization along the $x$ direction, parallel to the layer

$$\frac{\Delta R}{R} = 8\frac{\pi}{\lambda}\mathrm{Im}\left\{\frac{\Delta\varepsilon_{xx}(\omega)}{\varepsilon_{\mathrm{sub}}(\omega)-1}\right\}, \qquad (2)$$

where $\Delta\varepsilon_{xx}(\omega)$ is the component of the dielectric response tensor of the layer along the $x$ direction and $\lambda$ is the wavelength of light. In the case of a homogeneous layer with bulk optical response, $\Delta\varepsilon_{xx}(\omega)$ reduces to $d[\varepsilon(\omega)-1]$ where $\varepsilon(\omega)$ is the dielectric function of the material and $d$ the thickness of the layer; Eq. (2) is then identical to the one obtained in the so-called three-phase model [20,26]. Moreover, in the simple case of a substrate with a real dielectric function, $\Delta R/R$ is proportional to $d\mathrm{Im}[\varepsilon(\omega)]/\lambda$, therefore to the optical absorption of the film. This is the case for Ag in the Drude region (below approximately 3.7 eV), where the real part of the dielectric film is negative and much larger than the imaginary

part [17]; any absorption line of the film in this energy region should therefore be observed as a negative peak in $\Delta R/R$.

To compare the experimental spectra with the spectrum expected for silicene, the imaginary part of the dielectric function of silicene has been obtained from the absorption spectrum calculated by Matthes *et al.* [16] and the real part calculated using the Kramers-Kroenig relation [27]. The dielectric function of Ag is taken from Ref. [17], slightly modified to take into account the working temperature [28]. The result for a silicene layer onto Ag is shown in Fig. 3 and is completely different from the measured spectra. The first observation, considering the computed SDR spectrum shown in Fig. 3(b), is that, although the absorption of silicene is equal to 0.023 in the infrared (below 1 eV), the effect on the reflectance of silver is very small in this region. Indeed, the computed SDR signal is smaller than 0.002 below 1 eV and progressively approaches zero in the far infrared. It would therefore be difficult to experimentally determine such a small effect, as the accuracy of the measurements is not better than about 0.005 in our case. Measuring the optical absorption of such an Si film would demand, as it has been done for graphene, to be able to remove the Si overlayer and to deposit it onto a transparent substrate like glass, which appears nonfeasible for the Si/Ag system. The second observation is that the computed spectrum in Fig. 3(a) displays two clear minima related to the maxima of silicene absorption shown in Fig. 1: the first one around 2 eV due to the $\pi$-$\pi^*$ transition, the second one around 4.6 eV due to the next interband transition in silicene. Both minima are totally absent in the experimental spectra. This is in line with our experimental observations reported in the previous section that no change of shape is visible in the evolution of the signal for these photon energies at the coverage of 1 FC. Thirdly, the calculated signal is small around 3 eV (corresponding to the very small calculated absorption for silicene in this energy region, see Fig. 1), while our experimental data show that signal increases with the energy of light, for both polarizations. Finally, the computed spectrum does not reproduce the experimental derivativelike feature around 3.8 eV, but on the contrary displays a sharp negative peak. Actually, the SDR signal in this region and for higher energies depends strongly on the expected absorption for silicene, but also on the absorption and reflection of Ag, as the interband region for Ag starts at about 3.8 eV [17]. The presence of the Si atoms on the surface of Ag can modify the optical interband transitions in the vicinity of the Ag surface. The interplay between the optical responses of the Si layer and of the Ag surface at and above 3.8 eV would need a full calculation of the structure and of the optical response of the silicene layer on top of the Ag(110) surface. Consequently, the disagreement in the high-energy region is less significant than the disagreement observed below 3.5 eV, which corresponds to the Drude region for Ag.

At this point, a qualitative conclusion can be drawn from the comparison of the experimental spectra and the calculated one: the optical response of the Si SANR layer is different from the one expected for silicene. This is in line with the recent questioning about the silicene nature of the Si NRs grown on Ag(110) [7–9].

## V. DETERMINATION OF THE OPTICAL RESPONSE OF THE Si ×2 SANR LAYER

In order to go further, we derive the optical response of the Si SANR layer from the SRD spectra obtained at 1 FC. Because of the anisotropic geometry of the ×2 structure of this layer, its optical response should be described by a complex dielectric tensor, with a component perpendicular to the substrate surface and two components parallel to it, one being along the long dimension of the NRs and the other one along the short dimension. Moreover, it has been shown by x-ray diffraction that the formation of the NRs is associated with a reconstruction of the Ag surface beneath the Si layer [7], with two missing Ag rows per ×2 unit cell. Such reconstruction is expected to have some influence on the reflectance of Ag.

In a first step, we analyze this second effect, and we show that it is much smaller than the experimentally observed effect. To illustrate this, we consider the change of reflectance due to the formation of nanotrenches on the Ag surface. Anisotropic silver surfaces induce a modification of the reflectance, as it has been shown previously [29]. Two different calculations which can take into account such effect are considered. The first one is a change in the Drude parameters of the Ag dielectric function [30]. For bulk silver, the plasma frequency is $\hbar\Omega_p = 9.2$ eV, and the relaxation time of the conduction electrons $\tau$ is given by $\hbar\tau^{-1} = 0.021$ eV. The roughening of the surface due to the reconstruction is expected to increase the value of $\tau^{-1}$. The plasma frequency can also change, as it is related to the effective mass of the conduction electrons, which may depend on the crystalline quality of the surface. Figure 4(a) shows the results of such calculations, using drastic changes of these parameters: $\hbar\tau^{-1} = 0.21$ eV [labeled (1) in the figure], $\hbar\Omega_p = 10.2$ eV [labeled (2)] and $\hbar\Omega_p = 8.2$ eV [labeled (3)], with a depth of the modified Ag layer equal to 0.4 nm (approximately 2 Ag ML). Clearly, the effects are different and much smaller than those experimentally observed [the experimental spectra have been drawn again in Fig. 4(b), in the range 2–4.5 eV for a better visualization, and at the same vertical scale as in Fig. 4(a)]. The second way to take into account the possible presence of nanotrenches is to consider an Ag surface layer described by an effective dielectric function given by $\varepsilon_x = f\varepsilon_{\mathrm{Ag}} + (1-f)\varepsilon_{\mathrm{vac}}$ and $\varepsilon_y^{-1} = f\varepsilon_{\mathrm{Ag}}^{-1} + (1-f)\varepsilon_{\mathrm{vac}}^{-1}$ for the polarization parallel ($x$) and perpendicular ($y$) to the trenches [31]. Here, $f$ and $(1-f)$ are the relative fractions of the width of the Ag walls and of the trenches, considered as vacuum. The reflectance of such a structure can be calculated by use of Eq. (2), where $\Delta\varepsilon_{xx}(\omega)$ is replaced by $t(\varepsilon_x - 1)$, or by $t(\varepsilon_y - 1)$ with $t$ the thickness of the reconstructed Ag layer. The schematic in Fig. 4(a) shows the geometry of such a system, where $a$, the period of the nanotrenches, is much smaller than the wavelength $\lambda$ of the incident light. Figure 4(a) gives the result of such a calculation for $f = 0.5$ and $t = 0.4$ nm. The spectra are completely different for both polarizations. It is almost zero for a polarization parallel to the trenches (and merged with the horizontal axis within the scale of the figure), while it displays a sharp minimum around 3.5 eV [labeled (4)] for a polarization perpendicular to the trenches, due to the presence of a pole in $\varepsilon_y^{-1}$ and whose position depends on the value of $f$ (3 eV for $f = 0.8$; 3.7 eV for $f = 0.2$). In all cases, the results are again quite

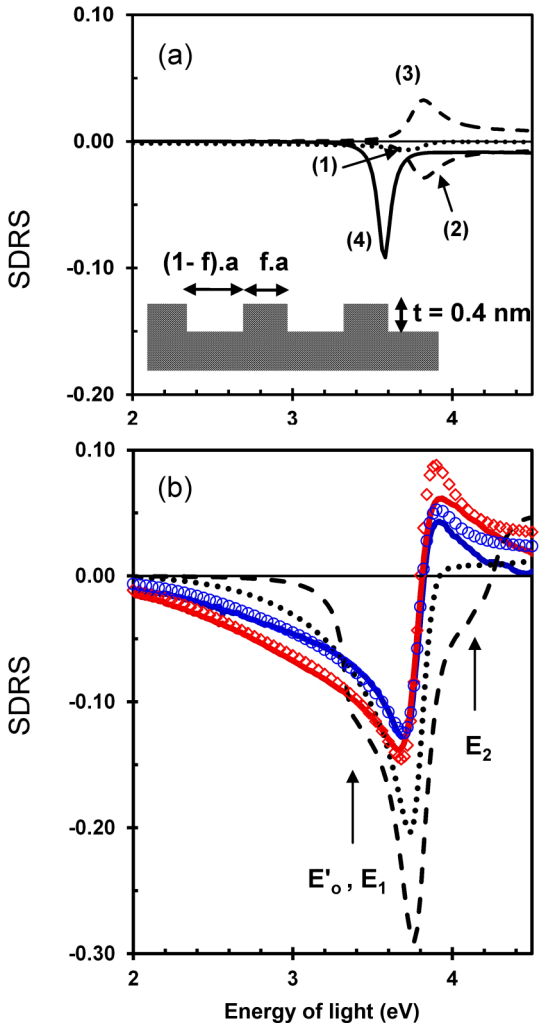


FIG. 4. (Color online) (a) Surface differential reflectance calculations for different surface dielectric functions of the Ag substrate (see text); the schematic shows the geometry used to calculate the effective dielectric function of the Ag nanotrenches; (b) SDR spectra measured for the Si SANR layer on Ag(110) [same as in Fig. 3(a)] with a zoom into the 2–4.5 eV region; red line: light polarization along $[1\bar{1}0]$; blue line: light polarization perpendicular to $[1\bar{1}0]$; black dashed line: calculation for 1 FC (0.8 ML) of crystalline Si; black dotted line: calculation for 1 FC of amorphous Si; red empty diamonds and blue empty circles: calculated curves with adjusted parameters (see text). Here, $E'_o, E_1$, and $E_2$ indicate the positions of the main critical points of crystalline Si [32,35].

different from the experimental spectra. These calculations show that the observed signal actually comes mainly from the optical response of the $\times 2$ Si SANR layer itself and not from the modification of the optical response of the Ag substrate caused by the Si-induced surface reconstruction.

In the second step, we compare the experimental SDR spectra for the SANR layer to the spectra calculated for crystalline silicon and for amorphous silicon with the same amount of silicon atoms (0.8 ML, i.e. an average Si thickness of 0.135 nm), using the dielectric functions of bulk materials [32,33]. The absorption of crystalline Si, shown in Fig. 1, is dominated by strong maxima corresponding to the direct interband transitions in crystalline Si at the $E'_o - E_1$ and $E_2$ critical points, located at 3.4 and 4.3 eV [32]. These transitions appear in the calculated SDR spectrum as negative features at the corresponding energies [Fig. 4(b)], together with the main sharp negative feature at 3.8 eV due to the Ag substrate. These features are not present in the experimental spectra. This shows unsurprisingly that the SANR layer does not display the optical properties of bulk Si crystal. Finally, the SDR spectrum calculated for an amorphous Si layer is also shown in Fig. 4(b). Although it does not reproduce correctly the experimental spectra, it has a general shape similar to them, but narrower. Consequently, this comparison between the experimental spectra and the one for amorphous silicon provides an interesting trail for further calculations.

The optical absorption of one layer of amorphous Si [33] is drawn in Fig. 1 as a dotted line [34]. Compared to the absorption of crystalline silicon, the amorphous one can be considered as resulting from a broadening of the optical transitions of the crystalline case accompanied by a small shift to the lower energies. Except for the well-defined absorption edge at 1.8 eV, below which absorption is zero, the absorption of amorphous Si can be reproduced correctly using a single Lorentzian function to describe its dielectric function

$$\varepsilon_L(\omega) = 1 - \frac{F_o^2}{\omega^2 - \omega_o^2 + i\omega\tau_o^{-1}}, \tag{3}$$

where $\hbar\omega_o = 3.8$ eV, $\hbar\tau_o^{-1} = 2.2$ eV, and $F_o = 15$ are the frequency, the inverse of the relaxation time, and the oscillator strength of the Lorentzian resonance. A similar description for the components parallel to the surface of the dielectric tensor of the SANR layer can be attempted to reproduce the experimental SDR spectra. However, the parameters are not completely uncorrelated, namely the relaxation time and the oscillator strength. For both polarizations, values for the inverse of the relaxation time ranging between 2.5 and 4 eV (and oscillator strength varying in opposite direction) lead to a reasonable agreement, and we fixed in the fitting procedure $\hbar\tau_o^{-1}$ equal to 2.5 eV, close and slightly higher than the value for amorphous Si. The calculated SDR spectra are displayed in Fig. 4(b) (red and blue empty symbols) and are actually very close to the experimental ones. The corresponding absorptions are shown in Fig. 1. The determined parameters are $\hbar\omega_o = 3.00$ eV, $\hbar\tau_o^{-1} = 2.5$ eV, and $F_o = 18.2$ for polarization along the NRs, while they are equal to $\hbar\omega_o = 3.19$ eV, $\hbar\tau_o^{-1} = 2.5$ eV, and $F_o = 15.4$ for a perpendicular polarization. The important point here is that the optical absorption of the SANR layer onto Ag(110) is dominated by an optical absorption of intensity similar to the one of amorphous Si, but shifted to smaller energies by an amount of about 0.6 to 0.8 eV. Consequently, the SANR Si layer does not display any indication of the $\pi \rightarrow \pi^*$ transition which is expected in the case of a partial $sp^2$ bonding and which should be observed at around 2 eV for silicene [16]. On the contrary, the optical absorption of the SANR layer is rather in agreement with a $sp^3$ bonding as in amorphous Si. For the well-ordered $\times 2$ layer, the broadening of the optical transition is likely not related to disorder, but rather to size effects: the sharp peaks in the optical absorption of crystalline Si are due to direct electronic transitions between almost parallel well-defined electronic bands [35]. Similarly,

the sharp absorption peak calculated at 2 eV for silicene is due to electronic transitions between the parallel filled $\pi$ and empty $\pi^*$ bands [16]. If the bands of the $\times 2$ Si layer are not as well defined or if they are not parallel, the interband transitions are expected to be smoothed out. This is the case, for example, for 1- to 3-nm Si nanocrystallites, whose optical response is almost identical to amorphous Si [36]. Finally, the observed energy shift of the main absorption feature with respect to bulk amorphous silicon is likely related to the different environment of the silicon atoms in the SANRs, due to the reduced dimension of the silicon layer and to the presence of the Si-Ag interface. It can also be noticed that the absorption is also larger for polarization along the NRs than perpendicular to them, which results from the anisotropic structure of the NRs.

## VI. CONCLUSION

We have conducted *in situ* optical measurements by means of surface differential reflectance spectroscopy for different amounts of Si deposited on Ag(110) at 450 K. The optical response at full Si coverage appears to be quite different than the one expected for a layer of silicene, derived by means of *ab initio* calculations. On the contrary, it is shown that it is well reproduced by use of a simple Lorentzian function to describe its dielectric function. This latter is very similar to the dielectric function of amorphous Si, but red-shifted by about 0.6 to 0.8 eV. This indicates that the SANR Si layer, which is well-ordered with a local $p(5\times2)$ or $c(10\times2)$ structure, likely does not display a partial $sp^2$ bonding but rather a $sp^3$ bonding as in amorphous Si. We hope that the reported optical response, thanks to comparison with future *ab initio* calculations, will help to determine the exact atomic structure of the Si SANR layer on Ag(110), in the current controversial debate concerning the formation of silicene on silver substrates.

## ACKNOWLEDGMENTS

The authors acknowledge Lars Matthes, Olivia Pulci, and Friedhelm Bechstedt for having provided the data file of the calculated absorption of silicene published in Ref. [16].

[1] H. Sahaf, L. Masson, C. Léandri, B. Aufray, G. Le Lay, and F. Ronci, Appl. Phys. Lett. **90**, 263110 (2007).
[2] B. Lalmi, H. Oughaddou, H. Enriquez, A. Kara, S. Vizzini, B. Ealet, and B. Aufray, Appl. Phys. Lett. **97**, 223109 (2010).
[3] A. Fleurence, R. Friedlein, T. Ozaki, H. Kawai, Y. Wang, and Y. Yamada-Takamura, Phys. Rev. Lett. **108**, 245501 (2012).
[4] L. Meng, Y. Wang, L. Zhang, S. Du, R. Wu, L. Li, Y. Zhang, G. Li, H. Zhou, W. A. Hofer, and H. J. Gao, Nano Lett. **13**, 685 (2013).
[5] A. Kara, S. Vizzini, C. Léandri, B. Ealet, H. Oughaddou, B. Aufray, and G. Le Lay, J. Phys.: Condens. Matter **22**, 045004 (2010); P. De Padova, C. Quaresima, C. Ottaviani, P. M. Sheverdyaeva, P. Moras, C. Carbone, D. Topwal, B. Olivieri, A. Kara, H. Oughaddou, B. Aufray, and G. Le Lay, Appl. Phys. Lett. **96**, 261905 (2010).
[6] P. Vogt, P. De Padova, C. Quaresima, J. Avila, E. Frantzeskakis, M. C. Asensio, A. Resta, B. Ealet, and G. Le Lay, Phys. Rev. Lett. **108**, 155501 (2012).
[7] R. Bernard, T. Leoni, A. Wilson, T. Lelaidier, H. Sahaf, E. Moyen, L. Assaud, L. Santinacci, F. Leroy, F. Cheynis, A. Ranguis, H. Jamgotchian, C. Becker, Y. Borensztein, M. Hanbucken, G. Prevot, and L. Masson, Phys. Rev. B **88**, 121411 (2013).
[8] S. Colonna, G. Serrano, P. Gori, A. Cricenti, and F. Ronci, J. Phys.: Condens. Matter **25**, 315301 (2013).
[9] P. Gori, O. Pulci, F. Ronci, S. Colonna, and F. Bechstedt, J. Appl. Phys. **114**, 113710 (2013).
[10] L. Matthes, P. Gori, O. Pulci, and F. Bechstedt, Phys. Rev. B **87**, 035438 (2013).
[11] L. Yang, J. Deslippe, C. H. Park, M. L. Cohen, and S. G. Louie, Phys. Rev. Lett. **103**, 186802 (2009).
[12] R. R. Nair, P. Blake, A. N. Grigorenko, K. S. Novoselov, T. J. Booth, T. Stauber, N. M. R. Peres, and A. K. Geim, Science **320**, 1308 (2008).
[13] K. F. Mak, M. Y. Sfeir, Y. Wu, C. H. Lui, J. A. Misewich, and T. F. Heinz, Phys. Rev. Lett. **101**, 196405 (2008).
[14] V. G. Kravets, A. N. Grigorenko, R. R. Nair, P. Blake, S. Anissimova, K. S. Novoselov, and A. K. Geim, Phys. Rev. B **81**, 155413 (2010).
[15] F. Bechstedt, L. Matthes, P. Gori, and O. Pulci, Appl. Phys. Lett. **100**, 261906 (2012).
[16] L. Matthes, O. Pulci, and F. Bechstedt, J. Phys.: Condens. Matter **25**, 395305 (2013).
[17] P. B. Johnson and R. W. Christy, Phys. Rev. B **6**, 4370 (1972).
[18] J. F. McGilp, Prog. Surf. Sci. **49**, 1 (1995).
[19] Y. Borensztein, Surf. Rev. Lett. **07**, 399 (2000).
[20] Y. Borensztein, T. Lopez-Rios, and G. Vuye, Phys. Rev. B **37**, 6235 (1988).
[21] Y. Borensztein, M. Roy, and R. Alameh, Europhys. Lett. **31**, 311 (1995).
[22] H. Proehl, R. Nitsche, T. Dienel, K. Leo, and T. Fritz, Phys. Rev. B **71**, 165207 (2005).
[23] C. Beitia, W. Preyss, R. DelSole, and Y. Borensztein, Phys. Rev. B **56**, R4371 (1997).
[24] R. Coustel, Y. Borensztein, O. Pluchery, and N. Witkowski, Phys. Rev. Lett. **111**, 096103 (2013).
[25] F. Manghi, R. Del Sole, A. Selloni, and E. Molinari, Phys. Rev. B **41**, 9935 (1990).
[26] J. D. McIntyre and D. E. Aspnes, Surf. Sci. **24**, 417 (1971).
[27] L. D. Landau and E. M. Lifshitz, *Electrodynamics of Continuous Media* (Addison-Wesley, Reading, MA, 1960).
[28] P. Winsemius, F. F. Vankampen, H. P. Lengkeek, and C. G. Vanwent, J. Phys. F **6**, 1583 (1976).
[29] Y. Borensztein, W. L. Mochan, J. Tarriba, R. G. Barrera, and A. Tadjeddine, Phys. Rev. Lett. **71**, 2334 (1993).
[30] M. Valamanesh, Y. Borensztein, C. Langlois, and E. Lacaze, J. Phys. Chem. C **115**, 2914 (2011).
[31] D. E. Aspnes, Thin Solid Films **89**, 249 (1982).

[32] D. E. Aspnes and A. A. Studna, Phys. Rev. B **27**, 985 (1983).
[33] D. E. Aspnes, A. A. Studna, and E. Kinsbron, Phys. Rev. B **29**, 768 (1984).
[34] The dielectric function of amorphous silicon actually displays some variation depending on the method of preparation. However, such variations affect only slightly the SDRS curve shown in Fig. 4(a).
[35] S. Adachi, Phys. Rev. B **38**, 12966 (1988).
[36] M. Losurdo, M. M. Giangregorio, P. Capezzuto, G. Bruno, M. F. Cerqueira, E. Alves, and M. Stepikhova, Appl. Phys. Lett. **82**, 2993 (2003).